JOURNAL OF GEOPHYSICAL RESEARCH, VOL. 107, NO. A10, 1272, doi:10.1029/2001JA009193, 2002

Radar observation of kinetic effects at meter scales for Farley-Buneman plasma waves

Christos Haldoupis
Physics Department, University of Crete, Iraklion, Crete, Greece

Kristian Schlegel
Max-Planck Institut für Aeronomie, Katlenburg-Lindau, Germany

Glenn C. Hussey and James A. Koehler
Institute of Space and Atmospheric Studies, Department of Physics and Engineering Physics, University of Saskatchewan, Saskatoon, Saskatchewan, Canada

Received 27 November 2001; revised 5 February 2002; accepted 27 March 2002; published 4 October 2002.

[1] Coherent backscatter Doppler measurements, made simultaneously at 144 MHz and 50 MHz from a common volume in the midlatitude *E* region ionosphere, were analyzed in order to study the phase velocity ratio of type 1 plasma irregularities at 1 m and 3 m wavelengths. In the analysis, high-resolution Doppler spectrograms were used first to identify the type 1 events and then to estimate the mean and spectral peak velocities from averaged power Doppler spectra. The simultaneous spectrogram signatures of type 1 echoes suggested a somewhat higher threshold for instability excitation at 144 MHz than at 50 MHz. Statistically, the measured 144 MHz to 50 MHz velocity ratios attain values above unity, mostly in the range from 1.05 to 1.14 with an overall average of 1.10. This 10% difference in the type 1 velocities at 144 MHz and 50 MHz was attributed to kinetic effects at short plasma wavelengths. For comparison, a linear kinetic model of the Farley-Buneman instability, which includes also a destabilizing plasma density gradient, was used to provide numerical estimates of type 1 phase velocities. It was found that the theoretical predictions for gradient-free Farley-Buneman waves agreed well with the observations, under the suppositions that the strongest type 1 echoes come from *E* region altitudes where conditions for instability are optimal and that type 1 waves have their phase velocities limited at threshold values equal to the plasma ion acoustic speed. The present study has confirmed the accuracy of the kinetic theory of the Farley-Buneman instability, which strengthens its validity and suitability for meter-scale *E* region irregularity studies. *INDEX TERMS:* 2471 Ionosphere: Plasma waves and instabilities; 2439 Ionosphere: Ionospheric irregularities; 2411 Ionosphere: Electric fields (2712); 2443 Ionosphere: Midlatitude ionosphere; 2437 Ionosphere: Ionospheric dynamics; *KEYWORDS:* Farley-Buneman instability, kinetic effects, ionospheric plasma waves, multifrequency E region backscatter, type 1 phase velocities

Citation: Haldoupis, C., K. Schlegel, G. C. Hussey, and J. A. Koehler, Observation of kinetic effects at meter scales for Farley-Buneman plasma waves, *J. Geophys. Res.*, *107*(A10), 1272, doi:10.1029/2001JA009193, 2002.

1. Introduction

[2] The linear theory of the Farley-Buneman (F-B) instability [*Farley*, 1963; *Buneman*, 1963], which has been studied and applied extensively over the last 40 years, is accepted as the plasma mechanism behind the so-called "type 1" *E* region echoes observed with coherent backscatter radars. Type 1 echoes are identified with magnetic aspect sensitive, mostly meter-scale, plasma waves which are excited spontaneously if the relative electron to ion drift velocity in the *E* region exceeds the plasma ion acoustic speed (e.g., see reviews by *Fejer and Kelley* [1980]; *Farley* [1985]; *Haldoupis* [1989]; *Sahr and Fejer* [1996]; and also the textbook of *Kelley* [1989]).

[3] The F-B instability has been treated within both the kinetic and fluid plasma theory frameworks. For example, in the original work Farley's theory was kinetic whereas Buneman employed the fluid equations. The fluid theory applies for plasma wavelengths considerably larger than the ion mean-free path $l_i = V_{ti}/\nu_i$ or the ion gyroradius $r_i = V_{ti}/\Omega_i$ (V_{ti} is the ion thermal velocity and ν_i, Ω_i are the ion neutral collision frequency and ion gyrofrequency, respectively). In practice this means that at *E* region altitudes, say between 100 and 115 km where the instability operates, the fluid model is valid for plasma wavelengths larger than a few meters [e.g., see also *Fejer et al.*, 1984]. At shorter wavelengths, the *E* region plasma gradually ceases to behave

0148-0227/02/2001JA009193$09.00

collectively and microphysical properties come into effect which can be accounted for only by kinetic theory.

[4] Compared to the kinetic approach, the F-B fluid theory is simpler and leads to a better physical insight through its analytical expressions for the angular frequency and growth rate of the waves. Because of this, the fluid model was used extensively over the years and was found, for all practical purposes, to be adequate down to irregularity scales of 1 m (e.g., see reviews by *Fejer and Kelley* [1980], *Farley* [1985], *Haldoupis* [1989]). On the other hand, although small, the kinetic effects must be present at shorter wavelengths if the existing kinetic theory models them accurately. In particular, the predicted rise in instability threshold with decreasing wavelength may be significant and thus experimentally resolvable. For example, Farley's kinetic theory predicts an instability threshold about 15% higher for 1 m than for 5 m plasma waves [e.g., see *Farley*, 1963, 1985]. Thus such differences could be identified and measured with a carefully designed multifrequency Doppler radar experiment.

[5] So far, there is limited experimental verification of the F-B instability kinetic effects at short wavelengths [*Leadabrand et al.*, 1965; *Balsley and Farley*, 1971; *Moorcroft and Ruohoniemi*, 1987; *Schlegel et al.*, 1990]. The present paper provides rare observational evidence showing the existence of such effects in meter-scale type 1 irregularities, which is in line with kinetic theory predictions. The observations were obtained with a dual VHF (very high frequency) radio Doppler experiment which viewed the unstable *E* region plasma at 144 MHz and 50 MHz and therefore was capable of detecting simultaneously type 1 echoes from plasma waves with 1.1 m and 3.1 m wavelength, respectively. The measurements were made in the midlatitude *E* region ionosphere where type 1 echoes are known to occur infrequently but with electric fields slightly above the instability threshold, that is, under conditions when the linear theory is applicable.

[6] In the sections to follow, the properties of midlatitude type 1 echoes are first outlined and then the dual-frequency Doppler experiment, on which the present study is based, is described. Next, the results of the present analysis are presented, which include typical examples and Doppler velocity statistics of type 1 echoes observed simultaneously at 144 and 50 MHz. Then, the experimental results are compared with numerical estimates obtained from the kinetic theory of the F-B instability, also with the inclusion of a destabilizing plasma density gradient. Finally, the physical reasons behind the theoretical predictions are discussed and the paper concludes with a summary of the main points.

2. Midlatitude Type 1 Echoes

[7] Type 1 irregularities occur regularly in the equatorial and auroral *E* regions because electric fields, which drive the F-B instability through $\mathbf{E} \times \mathbf{B}$ electron drifts, often attain values higher than the instability threshold [e.g., see *Fejer and Kelley*, 1980]. At midlatitude, ambient (dynamo) electric fields are well below the F-B threshold and thus the instability is unlikely to take place there. In spite of this however, the operation of SESCAT, the acronym for Sporadic *E* Scatter experiment, in Crete, Greece, has established that type 1 echoes can also occur at midlatitude during strongly unstable conditions inside sporadic *E* layers [*Schlegel and Haldoupis*, 1994; *Haldoupis et al.*, 1997]. This implies the existence at times of electric fields as large as 15 mV/m, at least an order of magnitude larger than expected. More recently, midlatitude electric fields up to about 20 mV/m were measured in situ during a rocket campaign in Japan [*Pfaff et al.*, 1998], and inferred from other radar experiments at 144 MHz [*Koehler et al.*, 1997], 52 MHz [*Huang*, 2000], and 30 MHz [*Hysell and Burcham*, 2000]. These relatively large **E** fields were interpreted as polarization fields set up inside dense sporadic *E* plasma patches with sharp horizontal conductivity gradients [*Haldoupis et al.*, 1996; *Tsunoda*, 1998; *Shalimov et al.*, 1998; *Cosgrove and Tsunoda*, 2001]

[8] Type 1 echoes last from several seconds to several minutes and constitute a small but distinct subset of midlatitude scatter. They have narrow Doppler spectra with peaks corresponding to wave phase velocities in the 250 to 350 m/s range, and average values about 15 to 20% lower than nominal *E* region ion acoustic speeds. This is probably because the ion acoustic speed, C_s, is reduced inside the sporadic *E* layer plasma by the abundance of heavy metallic ions, mostly Fe^+ [e.g., see *Schlegel*, 1985]. Often type 1 echoes are weak and appear in the spectrum together with the commonly observed broader spectral part centered at small Doppler shifts and attributed to "type 2" echoes [e.g., see *Fejer and Kelley*, 1980; *Haldoupis*, 1989], whereas at times type 1 echoes can dominate the spectrum or may appear in the absence of any type 2 spectral component. The observations support the notion of a velocity threshold for instability and suggest that type 1 echoes are most likely due to pure F-B waves, that is, there seems to be no plasma density gradient contribution in the instability process.

3. A Dual-Frequency Radio Scatter Experiment

[9] The experiment to be described here was designed to observe the wavelength dependence of meter-scale irregularities in the midlatitude *E* region ionosphere. In brief, two co-located continuous wave (CW) Doppler radars at 50 MHz and 144 MHz, with nearly identical antenna radiation patterns, were operated simultaneously to detect backscatter from the same region. The experiment took place in Crete, where the existing 50 MHz SESCAT Doppler system [e.g., see *Haldoupis and Schlegel*, 1993] was supplemented by a similar 144 MHz CW radar supplied by the University of Saskatchewan, for joint backscatter measurements from mid-June to mid-August 1996. The 144 MHz antenna arrays, which consisted of four 10-element Yagis, were scaled as closely as possible to the SESCAT 50 MHz arrays so as to have very similar beamwidths in order to observe the same *E* region volume.

[10] The experimental configuration and a few key parameters are summarized in Figure 1. Both systems were bistatic with the transmitter and receiver sites separated by 120 km along the northern coastline of Crete. The viewing volume in the *E* region was defined by the intersecting antenna radiation patterns and the strong magnetic aspect sensitivity of the echoing irregularities. The 3 dB ionospheric viewing area of about 15×20 km^2 was centered at about 30.8° geomagnetic latitude (L = 1.35) and 52.5°

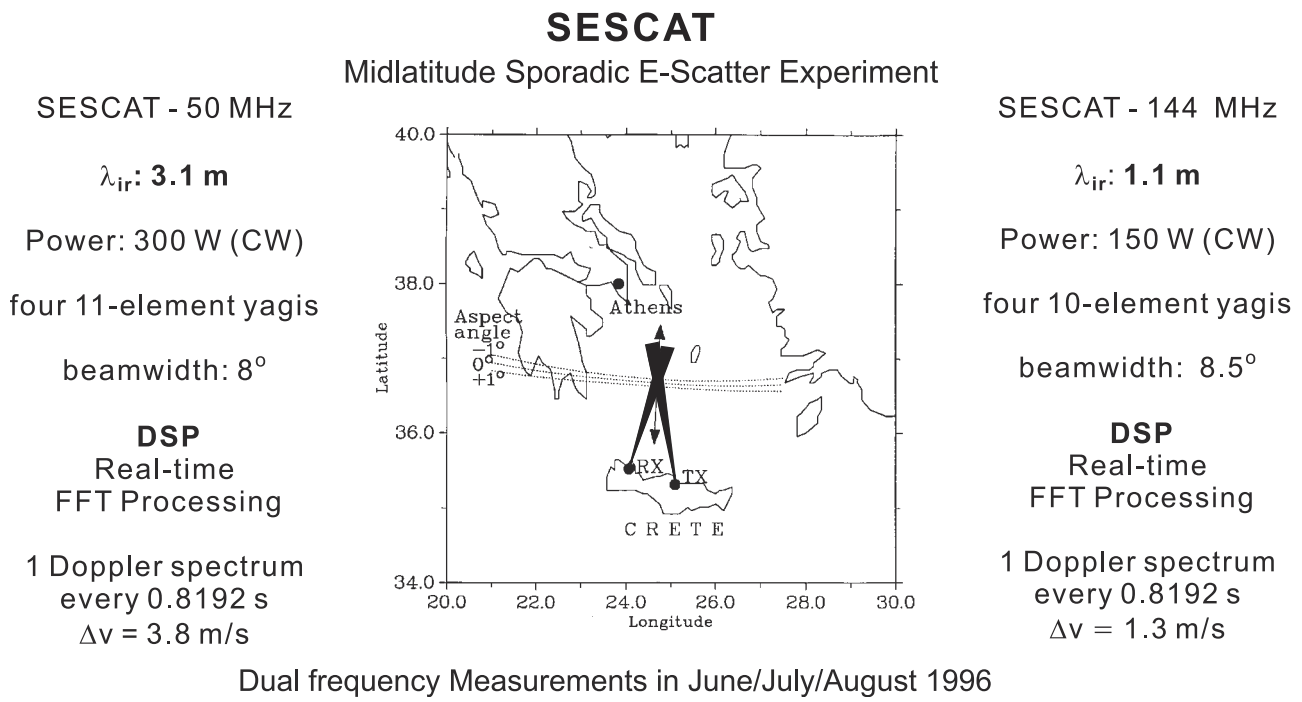

Figure 1. Location, observing geometry and technical information of the dual-frequency Doppler radar experiment relating to the present study. Its purpose was to observe simultaneously at 144 MHz and 50 MHz magnetic aspect-sensitive coherent backscatter from 1.1 m and 3.1 m plasma irregularities inside a common volume of the midlatitude *E* region ionosphere.

magnetic dip, and was located just to the east of the Aegean island of Milos. In this geometry the backscatter was caused by electrostatic plasma waves propagating along the bisector of the angle formed by the incident and the scattered radio waves, with wavelengths of 3.15 m and 1.10 m for 50 MHz and 144 MHz, respectively. Both receiver outputs were digitized and processed on site by using two identical digital signal processor (DSP) units housed in a personal computer. Special software was developed that allowed fast Fourier transformation and power computations to be performed in real time. Power spectra were calculated every 0.8192 s with a Doppler velocity resolution of 1.3 m/s and 3.6 m/s for the 144 MHz and 50 MHz backscatter, respectively.

[11] More experimental details and an overview of the observations are given by *Koehler et al.* [1997]. These demonstrated clearly for the first time the different character of type 1 and type 2 irregularities. Both irregularity types were observed at both frequencies, but the 144 MHz echoes were considerably weaker than those at 50 MHz. The 144 MHz type 2 waves were absent during times of weak to moderately strong 50 MHz echo occurrence and appeared only when the signal at 50 MHz became very strong with signal-to-noise ratios exceeding 20 dB; these differences between frequencies suggested a steep wave number spectrum in the wavelength range from 3 m to 1 m. On the other hand, and in sharp contrast to type 2 echoes, there was nearly one to one correspondence in the occurrence of type 1 echoes, even when the signal at 50 MHz was only a few decibels above noise. In a later study by *Koehler et al.* [1999], calibration procedures were applied in order to study the scattering cross-section ratios and the spatial spectrum. It was found that the *k*-spectrum is nearly 3 times steeper for type 2 than type 1 waves in the 3 m to 1 m irregularity wavelength range. The present paper, which comes as a continuation of this previous work, focuses on the simultaneous velocities of backscatter from 1 m and 3 m type 1 irregularities and how these velocities compare with kinetic theory.

4. Velocities of Type 1 Echoes at 144 and 50 MHZ

[12] During the two-month experimental campaign, several events of type 1 echoes were detected, having lifetimes from about 30 s to a few minutes. They were characterized by abrupt, threshold-like, appearances of backscatter and had narrow spectra with mean line-of-sight speeds exceeding 250 m/s. Also, they were observed mostly with motions away from the radar, that is, at negative Doppler shifts. Type 1 echoes with positive velocities were also seen but less often and with shorter lifetimes.

[13] A typical type 1 event is shown in Figure 2. Seen there are Doppler spectrograms observed at 144 MHz and 50 MHz and scaled to Doppler velocity instead of frequency shift in order to facilitate direct comparison between the two radio frequencies. The two spectrograms in Figure 2 look different, with the 50 MHz one being much busier. This is because of the low-velocity broad spectra associated with type 2 echoes, which tend to dominate the scatter at 50 MHz but not at 144 MHz. The type 2 echoes at 50 MHz and 144 MHz, which have been studied in detail by *Koehler et al.* [1997, 1999], are of no relevance to this study. Here we focus only on type 1 echoes which appear nearly always in both the 144 and 50 MHz spectrograms, although not always for the same duration.

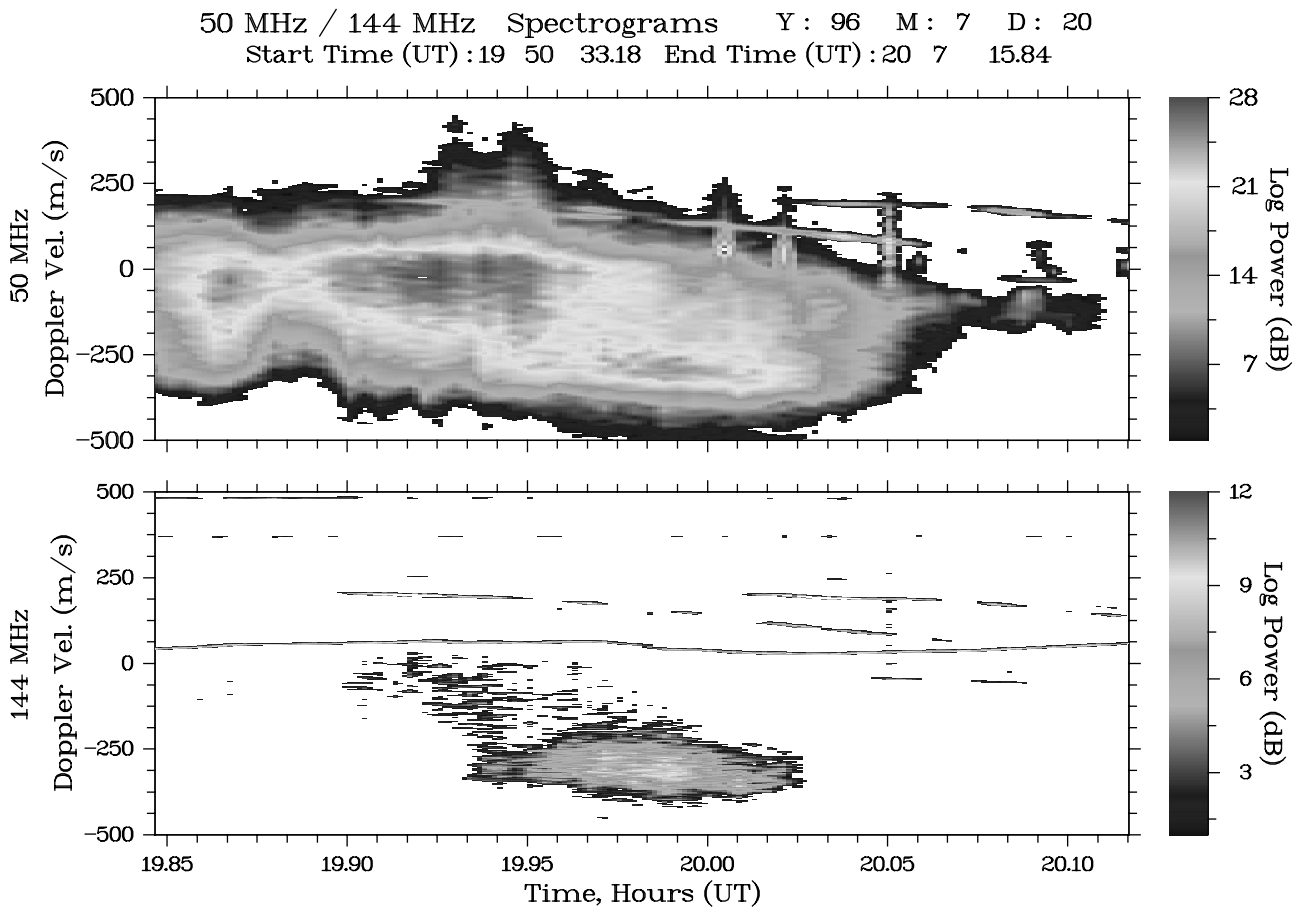

Figure 2. Simultaneous Doppler spectrograms of coherent backscatter at 50 MHz (top) and 144 MHz (bottom). Seen here is a typical event of type 1 echoes, characterized by large negative Doppler velocities and narrow spectra, seen concurrently in both radar frequencies. The time axis is in decimal hours UT (local time LT = UT + 1.6 hours). The long narrow lines are either due to antenna sidelobe airplane reflections or interference. Note also that type 2 echoes (broad spectra centered at lower Doppler shifts) dominate the spectrogram at 50 MHz but they are nearly absent at 144 MHz. See color version of this figure at back of this issue.

[14] The type 1 echoes in Figure 2 are present in both radio frequencies for about 6 min from ~19.93 to 20.03 decimal hours UT. They are marked by a narrow spectrum about a fairly constant Doppler velocity near 300 m/s, which is typical of midlatitude type 1 backscatter [e.g., see *Haldoupis et al.*, 1997]. Note that the type 1 spectral signature lasts longer at 50 MHz, since it extends in time prior and after the abrupt appearance of its 144 MHz counterpart. This may be attributed to a lower threshold for 3 m type 1 wave excitation as compared to 1 m waves.

[15] In the present study we are interested in comparing the type 1 velocities observed simultaneously at 50 and 144 MHz. To obtain a quantitative picture, we considered self-normalized power spectra averaged over about 10 s and smoothed further by a 5-point binomial filter. An example of such a spectrum pair is illustrated in Figure 3. As maybe seen, the 144 MHz type 1 spectrum (dashed line) is shifted to higher Doppler velocities by about 8% to 10% relative to the 50 MHz one (solid line). Inspection of many plots similar to Figure 3 indicated that the great majority of type 1 spectra at 144 MHz are centered systematically at somewhat higher Doppler velocities than those at 50 MHz.

[16] To quantify the differences between the 144 and 50 MHz type 1 velocities, we considered the Doppler velocity band of ±(200 to 400) m/s, and computed therein both the weighted mean velocity, V_{mean}, and the velocity at the spectral peak, V_{peak}. These estimates are taken to represent approximately the mean and most probable type 1 wave phase velocities. In making this correspondence, we are of course aware of possible offsets introduced by neutral wind components along the observing direction. These effects, however, which cannot be determined by our data alone, will affect equally the magnitude of the phase velocities of 1 m and 3 m waves.

[17] Figure 4 illustrates the times series of the V_{mean} and V_{peak} for the event shown in Figure 2. During the occurrence of type 1 echoes between about 19.93 and 20.03 decimal hours UT, both phase velocity estimates are systematically higher for the 1 m waves by 20 to 30 m/s relative to the 3 m waves. In general, this behavior was noted to prevail in nearly all type 1 events available in this study.

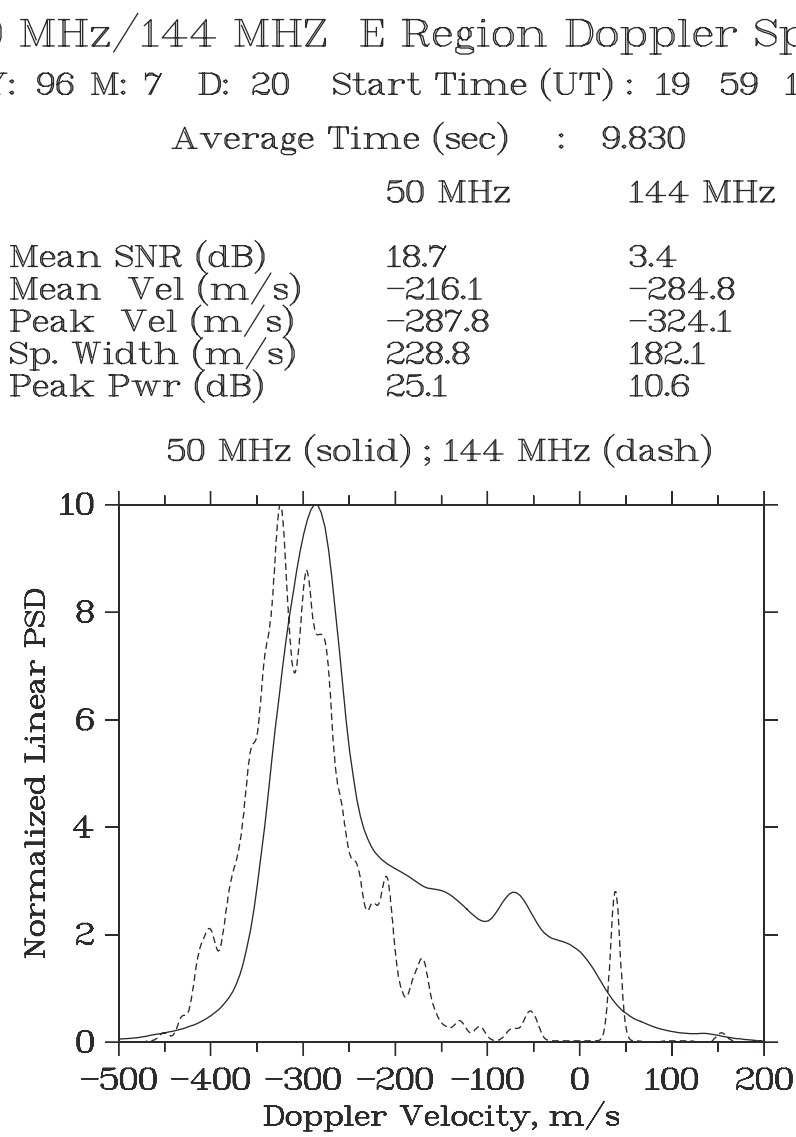

Figure 3. A typical example of a Doppler power spectrum pair of type 1 echoes detected simultaneously at 50 and 144 MHz. As seen, at 144 MHz (dash line) the type 1 spectrum is shifted by about 30 m/s (∼10%) in relation to that at 50 MHz (solid line). At 50 MHz the spectrum is a mixture of type 1 and type 2 echoes but not at 144 MHz.

[18] Figure 5 shows scatterplots, where all simultaneous 144 MHz versus 50 MHz type 1 velocity estimates are compared to each other. The top panels refer to V_{mean} whereas the bottom ones to V_{peak}. The open dots in the left-hand panels refer to type 1 echoes with negative Doppler shifts, whereas the solid dots in the right-hand panels refer to positive Doppler shifts. The positively shifted echoes represent a total of about 21 min of type 1 echo occurrence while the negatively shifted ones represent about 12 min. The diagonal solid lines in each figure represent positions of equal 144 MHz and 50 MHz velocities. The type 1 velocity estimates, either V_{mean} or V_{peak}, fall in the ±(250 to 350) m/s range and are systematically higher at 144 MHz than at 50 MHz.

[19] The histograms of the measured V_{mean} and V_{peak} velocity magnitudes are shown in Figure 6, in which both positive and negative Doppler shifts are included. The upper panel shows the superimposed mean velocity distributions of 50 MHz (solid line) and 144 MHz (dashed lines), whereas the bottom panel shows the corresponding peak velocity distributions. The 144 MHz velocity distributions are shifted to higher velocities by about 20 to 40 m/s relative to the 50 MHz ones. Shown also in the figure are the computed weighted means of the distributions which, on the average, show that type 1 velocities at 144 MHz are about 10% higher than at 50 MHz.

[20] Finally, Figure 7 shows the distributions of V_{mean} (upper panel) and V_{peak} (lower panel) velocity ratios of 144 MHz to 50 MHz type 1 echoes. Again, the histograms shown here are based on the total number of estimates for positively and negatively Doppler shifted echoes. Also printed at the left of each panel are the weighted mean and standard deviation of the histograms. By considering all distributions we conclude that the type 1 velocity ratios V_{144MHz}/V_{50MHz} take up

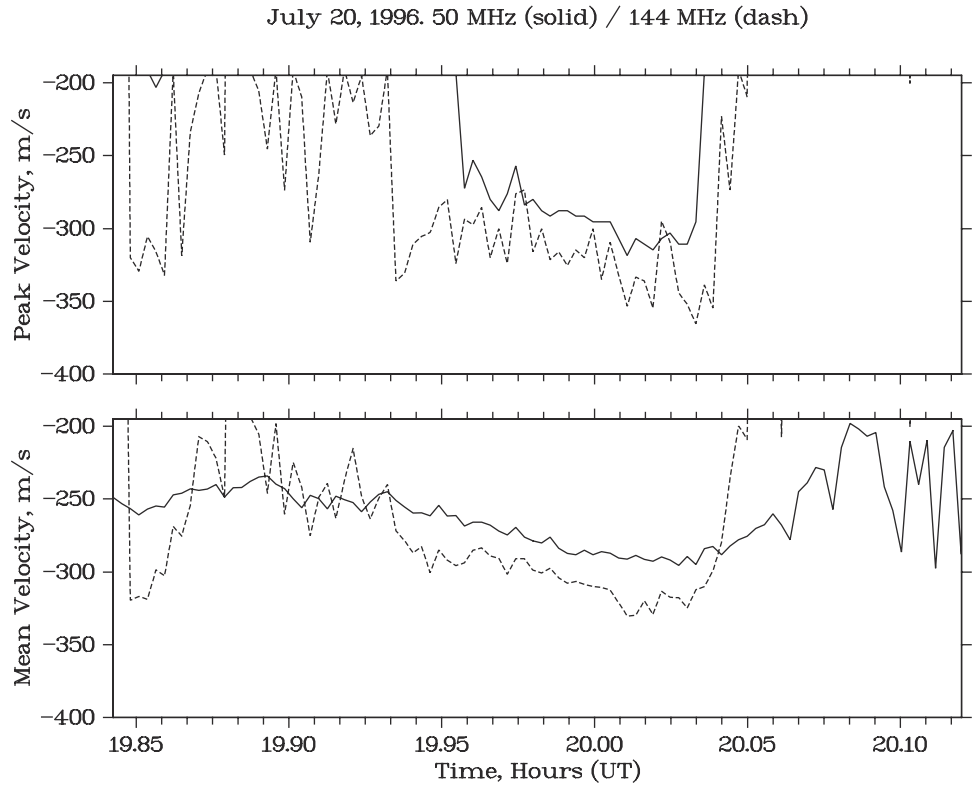

Figure 4. Weighted mean and spectral peak velocities in the −200 to −400 m/s spectral band, measured simultaneously at 50 MHz (solid line) and 144 MHz (dash line), shown for the same time interval as in Figure 2. As seen, these velocity estimates remain steadily higher at 144 MHz, in relation to those at 50 MHz, during the occurrence of type 1 echoes from about 19.94 to 20.04 decimal hours UT.

values systematically higher than 1.0. The mean velocity ratio ranges on the average between about 1.09 and 1.11.

5. Predictions of the Kinetic Theory

[21] In this section we apply the linear kinetic theory of the F-B instability at threshold conditions (marginal stability) in order to compare its predictions with our experimental findings. An alternative approach would have been to apply the generalized fluid theory of the F-B instability, developed by *Kissack et al.*, [1995], which incorporates in addition to the continuity and momentum equations the complete energy equation for the electrons. We believe that, for the purposes of the present short wavelength study, the kinetic theory is more suitable.

[22] In this comparison, we adopt the widely used supposition that the phase velocities of type 1 echoes are limited to instability threshold values. That is, they are close to C_s regardless of the driving electron-ion drift velocity magnitude. This has been inferred from many equatorial and auroral type 1 velocity measurements and is used widely in the literature (see reviews by *Fejer and Kelley* [1980], *Farley* [1985], *Haldoupis* [1989]; also see relevant studies of simultaneous *E* region backscatter and incoherent scatter electric field measurements by, e.g., *Nielsen and Schlegel* [1985] and *Haldoupis and Schlegel* [1990]). In our case, the $V_{phase} \simeq C_s$ assumption is likely to be valid anyway because at midlatitude the electric fields are small and thus are not expected to exceed the F-B threshold greatly. This implies that at midlatitude the instability is likely to operate not far above its threshold and under conditions when linear theory is approximately valid.

[23] The original kinetic theory of *Farley* [1963] was later extended to shorter wavelengths by considering additional finite Debye-length and electron Larmor-radius terms [*Lee et al.*, 1971], and generalized further to include a destabilizing plasma density gradient [*Schmidt and Gary*, 1973]. Since then, the theory has been developed further and used by several authors in the investigation of short-scale type 1 irregularities in both the equatorial and auroral electrojets [e.g., *Ossakow et al.*, 1975; *Schlegel and St.-Maurice*, 1983; *Schlegel*, 1983; *Moorcroft*, 1987, among several others].

[24] Here we use for computations the kinetic theory version given by *Schlegel* [1983] and *Schlegel and St.-Maurice* [1983]. The dispersion relation depends on the gyrofrequencies, the collision frequencies with the neutrals, and the temperatures for both the electrons and ions. It also depends on the instability driving terms, that is, the electron-ion drift velocity $\mathbf{V}_d = \mathbf{V}_e - \mathbf{V}_i$ (which at lower altitudes is taken nearly equal to the Hall electron drift $\mathbf{V}_e = \mathbf{E} \times \mathbf{B}/B^2$), and the electron density gradient ∇N_e. As discussed by *Moorcroft* [1987], for a given set of these parameters the real and imaginary part of the dispersion relation can be represented functionally as

$$fr(\omega, \gamma, k, \theta) = 0, \qquad fi(\omega, \gamma, k, \theta) = 0$$

where ω, γ and k are the plasma wave angular frequency, growth rate and wave number, respectively; θ is the

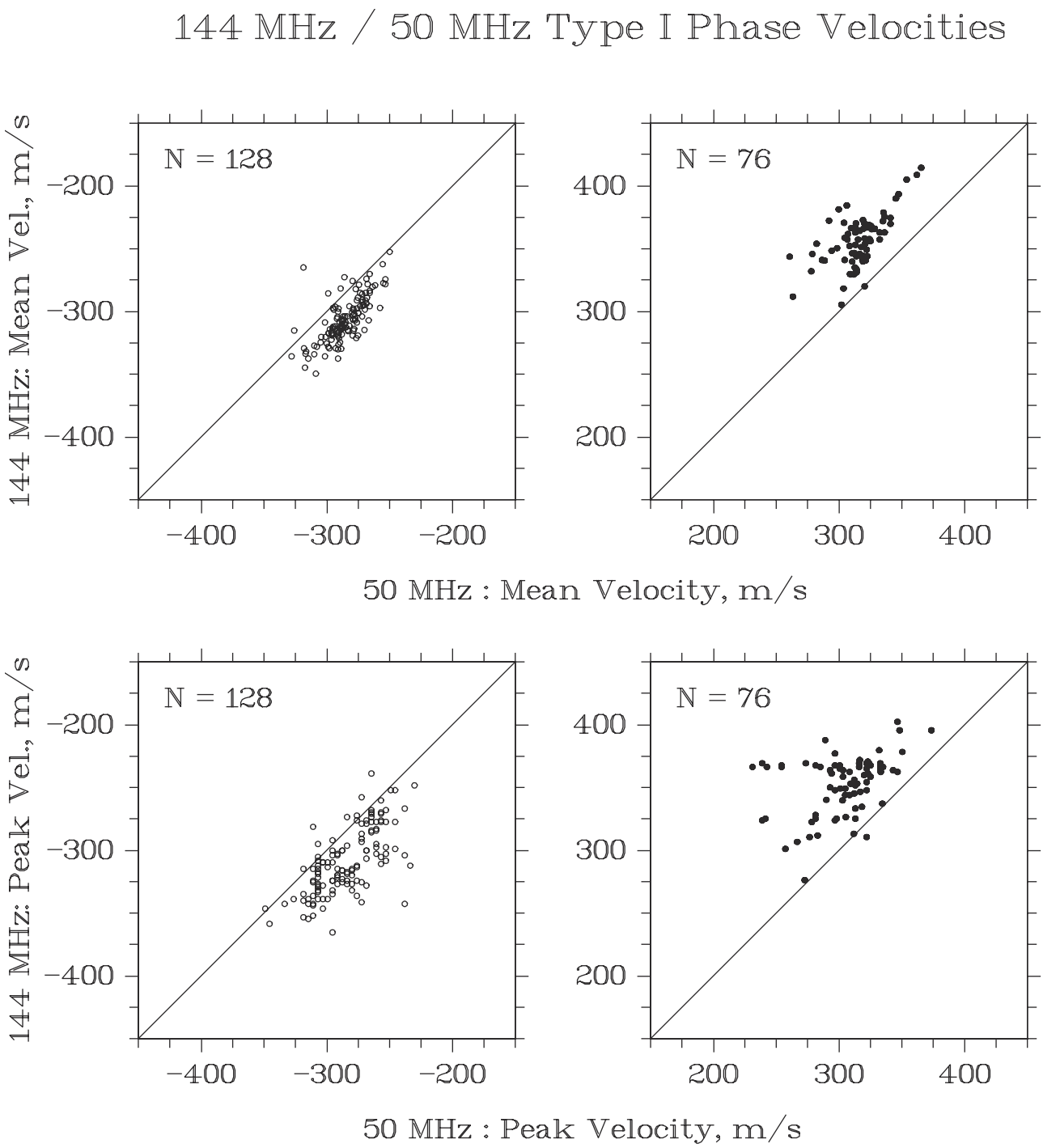

Figure 5. The mean (top panels) and peak (bottom panels) Doppler velocities at 144 MHz are plotted against those at 50 MHz for positively (right-hand panels) and negatively (left-hand panels) Doppler-shifted type 1 echoes. Mean and peak velocities remain steadily higher at 144 MHz than at 50 MHz.

magnetic aspect angle, that is, the angle between **k** and the direction perpendicular to the magnetic field. For a given k and θ these equations can be solved numerically to obtain ω and γ. The dispersion relation was solved by using the iterative computational procedure of *Schlegel and St.-Maurice* [1983].

[25] All calculations were carried out for the irregularity wavelengths of 1.10 m (144 MHz) and 3.15 m (50 MHz), which are probed in the Crete backscatter experiment. Typical E region plasma parameters were used which, for a given altitude, included the collision frequencies of electrons and ions with the neutrals, and the electron and ion temperatures. Since midlatitude backscatter relates closely to sporadic E layers [e.g., see *Hussey et al.*, 1998], a mean ionic mass m_i = 43 amu (atomic mass units) was adopted as representative of the metallic ion population, between the heavy Fe^+ ions (56 amu) and the lighter metallic ions like Si^+ (29 amu) and Mg^+ (24 amu) [e.g.,

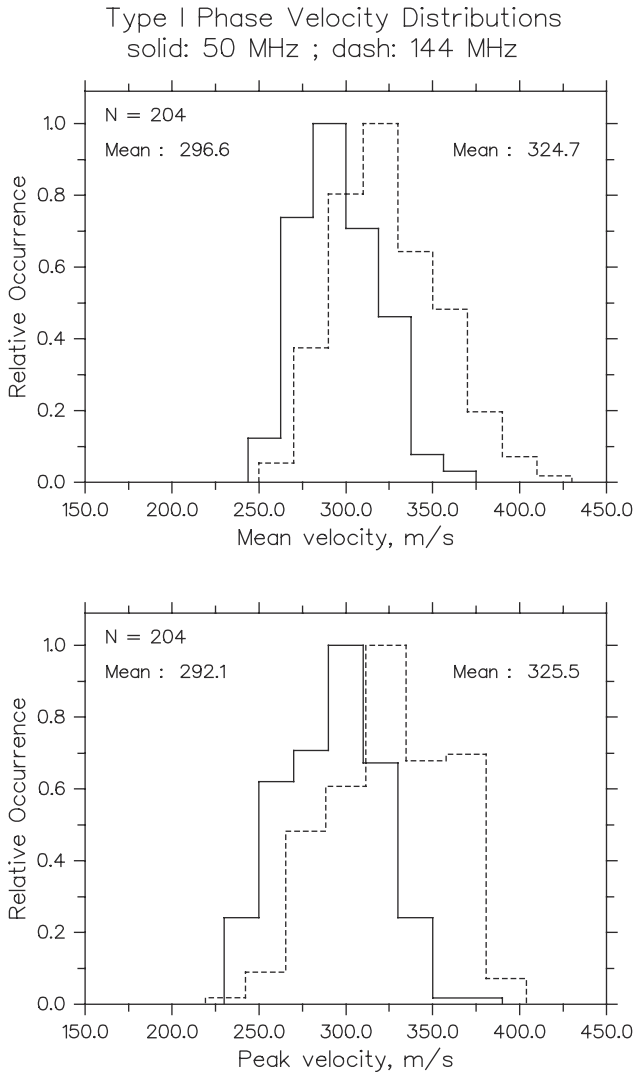

Figure 6. Normalized histograms (distributions of occurrence) of the estimated mean (top) and peak (bottom) velocities for 50 MHz (solid line) and 144 MHz (dash line) type 1 echoes.

see *Schlegel*, 1985]. As for the gyrofrequencies, we used $\Omega_e = 7.6 \times 10^6$ s^{-1} and $\Omega_i = 133$ s^{-1}, with the magnetic field at the SESCAT field of view taken as equal to 0.43 G. Finally, the excited plasma waves are assumed to propagate almost perpendicular to the magnetic field and to have phase velocities equal to those at instability threshold, which implies that all calculations were carried out for $\gamma \simeq 0$ and $\theta \simeq 0°$. This allowed the estimation of ω and subsequently of the wave phase velocity $V_{ph} = \omega/k$ at threshold, as well as the threshold electron drift velocity V_{th}, or alternatively the threshold electric field $E_{th} \simeq V_{th}B$.

[26] The kinetic theory results in the absence of an electron density gradient are summarized in Figure 8 for altitudes between 95 and 115 km. As seen from the upper panel, the threshold electric field always remains greater for 1.10 m waves than for 3.15 m, with this difference becoming maximum between 104 and 106 km where the conditions for instability become optimal. There, E_{th} attains its minimum values near 13.5 mV/m and 15 mV/m for the 3.15 m and 1.10 m wavelengths, respectively. Note that below about 100 km E_{th} experiences a steep increase because of large increases in the collision frequencies of the charged particles with the neutrals at lower altitudes. In upper altitudes the instability threshold increases again but more gradually, because of higher C_s values caused by the increase in the particle temperatures with height, combined also with the diminishing role of collisions with increasing altitude; also, another contributing factor to the increase in threshold electric field with height is the increasing ion velocity as the ions become increasingly magnetized.

[27] As mentioned, the objective here is to compare the observed type 1 velocities at 144 and 50 MHz with the kinetically predicted phase velocities at instability threshold for the 1.10 m and 3.15 m F-B plasma waves. The theoretical predictions are shown in the mid and lower panels of Figure 8. The phase velocity at threshold is always higher for 1.10 m waves than for the 3.15 m ones. The difference between the phase velocities increases with

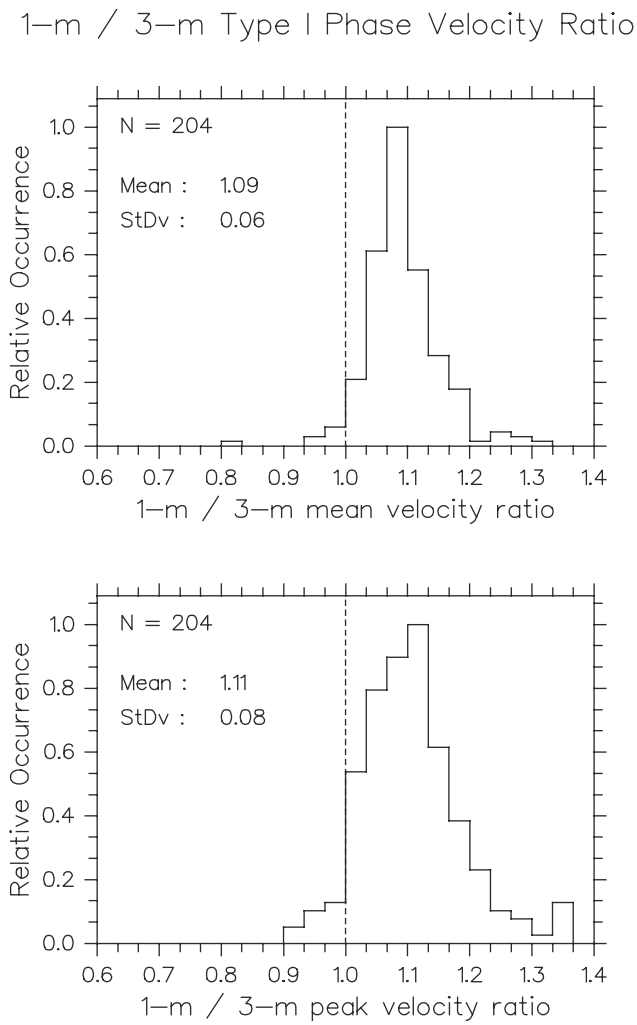

Figure 7. Normalized histograms (distributions of occurrence) of the mean (top) and peak (bottom) velocity ratios of 144 MHz to 50 MHz type 1 echoes. The distributions show that type 1 velocities at 144 MHz are on the average about 10% higher than at 50 MHz.

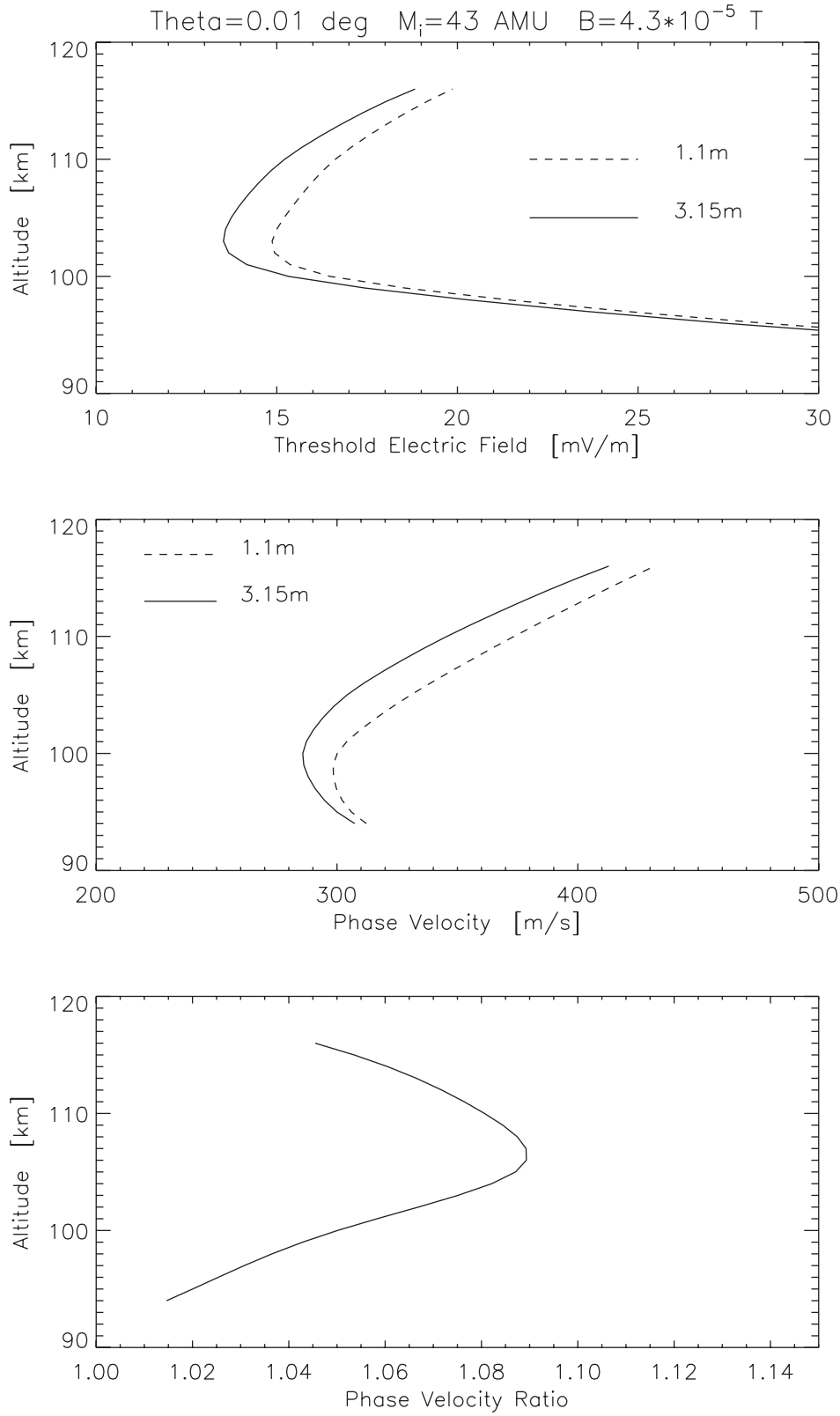

Figure 8. Marginal stability (threshold) predictions of the kinetic theory of Farley-Buneman instability for 1.1 m and 3.15 m plasma wavelengths, corresponding to 144 MHz and 50 MHz backscatter, respectively. The numerical results are computed for plasma density gradient-free conditions and for waves propagating almost perpendicular to the magnetic field inside midlatitude sporadic *E* (metallic ion) plasma. The upper panel refers to the required electric field threshold, the mid panel to the wave phase velocities and the lower panel to the 1.1 m to 3.1 m phase velocity ratio. Note that the conditions for instability are optimal at about 104 to 105 km altitudes.

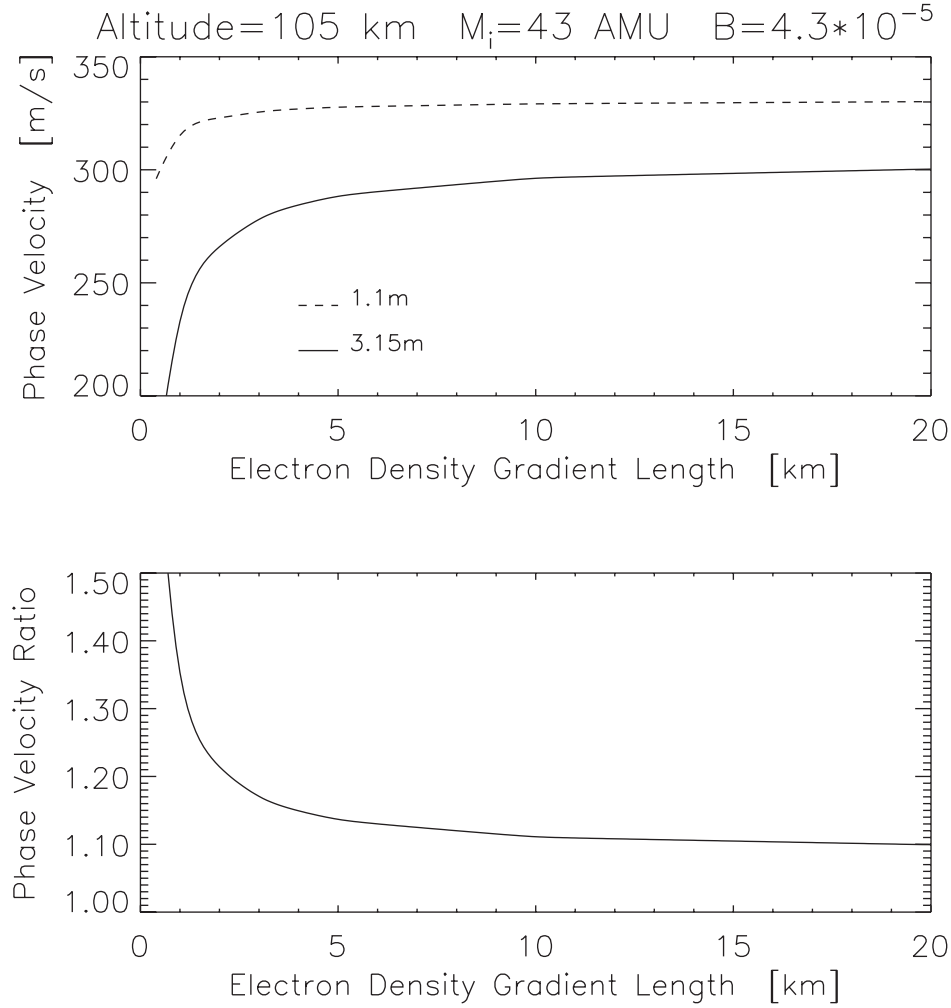

Figure 9. Threshold predictions at 105 km altitude, of the Farley-Buneman instability kinetic theory for the phase velocities of 1.1 m and 3.15 m plasma waves (top) and their ratio (bottom), as a function of a (destabilizing) plasma density gradient length.

altitude up to about 105 km and then decrease again, a behavior that is to be discussed later. If we take only the optimal heights for instability, say between 104 and 106 km, then the predicted threshold velocities there are about 315 m/s and 290 m/s for the 1.10 m and 3.15 m wavelength waves, respectively, while their phase velocity ratios are near 1.09. These values compare quite well with the observed mean phase velocities at 144 MHz and 50 MHz and their ratios, which were found to be about 325 m/s, 295 m/s and 1.10, respectively.

6. Possible Effects of a Destabilizing Density Gradient

[28] The theoretical predictions in Figure 8 refer to pure F-B waves where there was no contribution of an electron density gradient in the excitation of the instability. Although the observations of midlatitude 50 MHz type 1 echoes support this postulation [e.g., see *Schlegel and Haldoupis*, 1994; *Haldoupis et al.*, 1997], possible density gradient effects on instability excitation cannot be ruled out entirely. As shown first by *Farley and Fejer* [1975], a destabilizing electron density gradient perpendicular to the magnetic field and parallel to the electric field could lower the instability threshold, and hence the observed phase velocities, to an extent that depends on the plasma wavelength. This threshold reduction is higher at longer than at shorter wavelengths. That is, a destabilizing plasma density gradient acts in the same direction as the kinetic theory effects do to lower the instability threshold of longer meter-scale waves more, relative to shorter ones.

[29] In order to judge if density gradient effects are significant in the dual-wavelength phase velocity measurements, similar kinetic theory calculations were performed but in the presence of a destabilizing plasma density gradient. The latter is characterized by a gradient length $L_N = N_e\ (dN_e/dx)^{-1}$ along the ambient electric field perpendicular to B, where N_e is the mean electron density. The numerical results for this case, computed at the optimal altitude of 105 km, are presented in Figure 9. The upper panel shows the phase velocity at threshold as a function of L_N for both wavelengths, whereas the lower panel shows the 1.10 m to 3.15 m phase velocity ratio also as a function of L_N.

[30] Figure 9 suggests that the measured type 1 mean velocities and their ratio can be approached only for large gradient lengths L_N, exceeding say values of 15 to 20 km. But, large L_N means a small and, for short wavelengths, rather insignificant density gradient effect. This reinforces the assumption of dealing with pure F-B waves because, as shown in Figure 8, almost the same velocity ratio near 1.09 was predicted at 105 km by the theory in the absence of any density gradient. On the other hand, although it cannot be proved by our data alone, L_N larger than, say 10 to 15 km, are not likely to exist during backscatter conditions. This is because the ambient electron density gradients during unstable conditions at midlatitude result from very steep vertical gradients in sporadic *E* layers. Thus gradient lengths perpendicular to **B** are expected to take values below say 1 to 3 km, which is in line with what is quoted often in the literature [e.g., *Ecklund et al.*, 1981; *Riggin et al.*, 1986, and several others]. As seen from Figure 9, these L_N values associate with phase velocity ratios $V_{1.1m}/V_{3.1m}$ greater than 1.15 to 1.20, which depart from the observations.

[31] In view of the arguments above, we conclude that there seem to be no significant effects in instability threshold reduction attributable to a destabilizing plasma density gradient. Thus, the observed velocity ratios V_{144MHz}/V_{50MHz} relate, very likely, with pure Farley-Buneman waves.

[32] On the other hand, the lack of density gradient effects on the observed type 1 irregularities points to the possibility of a serious discrepancy between theory and observations. This arises because, during E_s backscatter conditions, sharp destabilizing electron density gradients are expected to exist, which should lower the threshold phase velocity below C_s in accordance with the linear theory [e.g., *Farley and Fejer*, 1975]. Instead, the observed velocities are near ion-acoustic speed values which implies an apparent disagreement with conventional theory. This implication is not new, as similar problems occur at high-latitude HF backscatter, where type 1 echoes with velocities near C_s are routinely observed [e.g., see *Milan and Lester*, 2001; *Lacroix and Moorcroft*, 2001] in spite of the fact that plasma density gradients must be of importance in those observations. A possible explanation may be found in the new "blob" theory of *St.-Maurice and Hamza* [2001], where the effects of gradients become negligible with wave growth, provided that the electric field is sufficient to generate an instability in the absence of a (favorable) gradient. We believe that this issue is of importance and deserves attention and a careful investigation.

7. Discussion

[33] To our knowledge, the only multifrequency radar experiment of relevance to our study was performed 30 years ago in the equatorial electrojet by *Balsley and Farley* [1971]. They made simultaneous Doppler spectrum measurements from the same *E* region volume in three frequencies: 16.25, 49.92 and 146.25 MHz. Their VHF observations, which compare directly to ours, were based on three daytime events of backscatter when westward propagating type 1 waves are seen routinely in the equatorial electrojet. As in our study, they always observed type 1 echoes in both radar frequencies and measured systematically higher mean velocities at 146 MHz than at 50 MHz. They reported 146 MHz to 50 MHz velocity ratios for the type 1 spectral peaks ranging from 1.07 to 1.15 and quoted an average velocity ratio of 1.10, which is very much in line with our observations. This remarkable agreement reinforces the reliability and representability of both their equatorial and our midlatitude type 1 echo measurements. *Balsley and Farley* [1971] attributed their observed 10% difference in the type 1 velocities at 146 MHz and 50 MHz to short wavelength kinetic effects as modelled by the theory of *Farley* [1963].

[34] Next, we discuss the possible physical reasons behind the observed increase in phase velocity, V_{ph}, with decreasing irregularity wavelength, λ. Given that the phase velocities of type 1 waves take up values equal to the plasma ion-acoustic speed, *Balsley and Farley* [1971] attributed the differences in V_{ph} as being mainly due to increases in C_s with decreasing λ. Although C_s is not a natural parameter as in the fluid theory, it enters indirectly into the kinetic equations through the Maxwellian distribution of the charged particles. The ion acoustic speed

$$C_s = \sqrt{\frac{K_B(\gamma_i T_i + \gamma_e T_e)}{\langle m_i \rangle}}$$

(where K_B is the Boltzmann constant, T_i, T_e are the ion and electron temperatures, and $\langle m_i \rangle$ is the mean ionic mass), will depend on wavelength through the specific heat ratios γ_i and γ_e for the ions and electrons. Given a plasma wave frequency ω and wavelength λ, the charged particles gain or lose energy by remaining within a wave compression or rarefaction. In simple terms, the particles are considered isothermal if they become fully thermalized with the neutrals through collisions during the period of the wave. Otherwise, they may be partly isothermal and partly adiabatic, or fully adiabatic if there is no energy exchanged with the neutrals.

[35] In the conventional fluid theory, the specific heat ratios are taken to be independent of wavelength and often are set equal to unity, implying that both charged species behave isothermally. This, however, may not be true at shorter scale lengths, because, as put by *Balsley and Farley* [1971]: "the electron and ion motions will be approximately isothermal at some wavelengths and approximately adiabatic in others", a situation that is expected to be automatically accounted for only by a complete kinetic theory. The conventional kinetic theory of the F-B instability, which was also applied in the present study, models reasonably accurately only ion-neutral collisional effects but it is approximate with respect to the electrons by forcing them to be isothermal. This means that the kinetic theory considers $\gamma_e \simeq 1$, therefore the dependence of C_s on λ can only be attributed to γ_i.

[36] The issue of whether the electrons are isothermal or adiabatic for meter-scale waves is complex and seemingly controversial. For example, *Farley and Providakes* [1989] used qualitative arguments to suggest that, for most situations of interest and because of the long cooling rates involved, electrons can be nearly adiabatic with 3 degrees of freedom, that is, $\gamma_e = 2/3$. On the other hand, *Kissack et*

al. [1997] used a rigorous fluid theory to show that these arguments break down because of thermal effects, and that γ_e takes a range of values depending on wavelength, magnetic aspect angle, electron and ion temperatures, and the electron-neutral collision frequency. Actually, the theory of *Kissack et al.* [1997] predicts γ_e values close to 1.0 for both 1 m and 3 m waves propagating perpendicular to **B** and for plasma conditions which are applicable to midlatitude *E* region. This result, which was interpreted as that the electrons control their own temperature and thus behave isothermally, is in agreement with the $\gamma_e \simeq 1$ approximation adopted in the kinetic theory of the F-B instability.

[37] With respect now to the massive ions, and because of the large energy exchange in elastic collisions with the neutrals, it is reasonable to consider that ions act more isothermally ($\gamma_i = 1$), especially at lower altitudes where $\nu_i \gg \omega$ and $l_i \ll \lambda$. Although the isothermal approximation for the ions is widely used in the literature [e.g., *Fejer and Kelley*, 1980; *Kissack et al.*, 1997], it may not be fully valid for short wavelengths at altitudes where ν_i becomes comparable to the plasma wave frequency ω. As shown by *Stubbe* [1989] in a rigorous kinetic treatment of *E* region electrostatic waves, the specific heat ratio for the ions can take values between 1 (isothermal) and 3 (adiabatic particles with one degree of freedom), depending on how the plasma wave frequency compares with elementary collisional effects of momentum transfer, energy transfer, and isotropization rates at different irregularity scales. As *Stubbe* [1989] shows, the ions are isothermal ($\gamma_i = 1$) when $\nu_i \gg \omega$ and adiabatic with $\gamma_i = 3$ when $\nu_i \ll \omega$, whereas for the case when ν_i and ω are comparable the ions may be partially isothermal and partially adiabatic, that is, $1 < \gamma_i < 5/3$. It is important to stress that the kinetic theory is taking into account these ion effects.

[38] We now apply the above, rather simplified, line of reasoning to the wavelengths of 1.1 m and 3.15 m, which are of interest to this study. First, by taking a typical phase velocity of 300 m/s for type 1 waves we estimate: $\omega_{1m} \sim 1.7 \times 10^3$ s^{-1} and $\omega_{3m} \sim 6.0 \times 10^2$ s^{-1}, corresponding to periods: $T_{1m} \sim 3$ ms and $T_{3m} \sim 10$ ms. On the other hand, ν_i ranges from about $1.2 \times 10^4\, s^{-1}$ at 95 km to $1.9 \times 10^3\, s^{-1}$ at 105 km and to $4.2 \times 10^2\, s^{-1}$ at 115 km. Next, by comparing ν_i to both ω_{1m} and ω_{3m}, we conclude that at lower altitudes, where $\nu_i \gg \omega_{1m}, \omega_{3m}$, the ions are nearly isothermal for both, 1 m and 3 m waves and thus $v_{ph}(1m) \simeq V_{ph}(3m)$ because $C_s(1m) \simeq C_s(3m)$. As the altitude increases however, the ions are expected to gradually become less isothermal and more adiabatic, in response to the decrease in collision frequency ν_i relative to plasma wave frequencies ω. This tendency is certainly more effective for 1 m wavelength waves than for 3 m ones, because in the latter case the period of the wave is larger. As a result, the ions can undergo more collisions with the neutrals within a wave period and therefore they behave less adiabatically at larger than shorter scales. Consequently, C_s will be somewhat larger for 1 m waves than for 3 m waves, because $\gamma_i(1m) > \gamma_i(3m)$, and so will the corresponding F-B phase velocities at threshold. The above physical arguments reconcile well with the kinetic theory estimates shown in Figure 8, where the required thresholds for instability and the phase velocity estimates at threshold are steadily higher for 1 m waves than for 3 m waves throughout the entire altitude range under consideration, that is, from 95 to 115 km.

[39] This interpretation is in line with suggestions made by *Schlegel* [1983] in his kinetic treatment of meter-scale waves, which was also used in the present study. There, he identified the ratio of wave frequency to ion-neutral collision frequency, ω/ν_i, as the most likely factor behind the dependence of type 1 phase velocities on wavelength. In fluid theory, the ratio ω/ν_i is required to be rather small, which agrees only for long wavelengths for which there is agreement between kinetic and fluid theory. This requirement however, becomes less and less valid with decreasing wavelength, leading to an increasing departure between the fluid and kinetic theory predictions for the phase velocity, with a corresponding spread between the phase velocities of 50 MHz and 144 MHz type 1 echoes.

[40] Finally, there is still an interesting theoretical trend in Figure 8 that needs to be mentioned. This relates to the altitude dependence of phase velocity difference $\Delta V_{ph} = V_{ph}(1m) - V_{ph}(3\ m)$. As seen, ΔV_{ph} increases steadily with altitude up to about 105 km, where it attains a maximum, and then starts decreasing. This behavior is depicted clearly by the change of $V_{ph}(1m)/V_{ph}(3m)$ ratio with altitude, shown in the lower panel of Figure 8. In view of our previous discussion, this implies that the tendency for the ions to become more adiabatic at shorter scales (1.1 m) than at longer ones (3.1 m) has to be a non-monotonic function of altitude. Then, the behavior of the $V_{ph}(1m)/V_{ph}(3m)$ ratio with altitude might be tentatively understood, if the effective γ_i values for 1 m and 3 m waves are gradually converging at higher altitudes as ν_i becomes increasingly smaller relative to both, ω_{1m} or ω_{3m}. Unfortunately, there is no altitude information in our experiment which would have allowed us to test this interesting theoretical prediction.

8. Summary and Conclusion

[41] In this paper, midlatitude *E* region backscatter measurements made simultaneously at 144 MHz and 50 MHz were analyzed in order to study how the phase velocities of type 1 plasma irregularities at 1.1 m and 3.1 m wavelengths compare to the predictions of the Farley-Buneman instability kinetic theory. Our motivation was to test the accuracy of the kinetic theory itself. The main results are summarized as follows:

1. The 144 MHz type 1 echoes required a somewhat higher threshold for excitation, and thus lasted for shorter lengths of time relative to those at 50 MHz. Statistically, the mean velocity at 144 MHz was ~325 m/s, about 30 m/s higher than at 50 MHz. The velocity ratio of 144 MHz to 50 MHz type 1 echoes ranged from about 1.06 to 1.14, with an overall mean value near 1.10. In other words, the phase velocities of 1.1 m type 1 irregularities were found to be on the average about 10% higher than at 3.1 m. The velocity differences of type 1 echoes at 144 MHz and 50 MHz were attributed to kinetic effects which are known to intensify at short wavelengths.

2. To compare the observations with theory, a linear kinetic model of the Farley-Buneman instability was used to compute numerical estimates of the phase velocities at threshold for 1.1 m and 3.1 m plasma waves. A very good

agreement was found between the observations and the kinetic theory predictions, under the postulations that type 1 echoes: a) are due to pure Farley-Buneman waves that originate mostly from *E* region heights where instability excitation is optimal, and b) have phase velocities limited at instability threshold values. The theory predicts about 9% higher threshold phase velocities for 1.1 m waves relative to 3.1 m waves, which agrees well with the 10% difference measured by the experiment.

3. In order to examine whether or not an ambient density gradient plays a greater role in lowering the instability threshold for 144 MHz than for 50 MHz echoes, phase velocities for 1.1 m and 3.1 m waves were again computed kinetically as a function of a destabilizing plasma density gradient. It was shown that for the gradient lengths anticipated in midlatitude, the predicted velocity ratios departed significantly from the measured values. This has reinforced the conviction that the observed type 1 echoes related to pure Farley-Buneman waves, and thus the measured differences in phase velocity are due to kinetic effects at short wavelengths. On the other hand, this observation casts some doubt about the density gradient role on primary wave generation as modelled by the conventional theory.

[42] In conclusion, the measured 144 MHz to 50 MHz velocity ratios of type 1 echoes were found to be in good agreement with the kinetic theory of the F-B instability, which predicts that the phase velocity of meter-scale plasma irregularities should increase slightly with decreasing wavelength. Physically, this was attributed to the differences of specific heat ratios for the ions with irregularity wavelength for meter-scale waves in the *E* region plasma, especially at altitudes where the conditions for instability are optimal. The present experimental verification of the anticipated, short-scale, kinetic effects of the Farley-Buneman theory confirms the accuracy of the theory and thus strengthens its validity as the key instability mechanism in the *E* region ionospheric plasma.

[43] **Acknowledgments.** This work was completed with support from the European Office of Aerospace Research and Development (EOARD), Air Force office of Scientific Research, Air Force Research laboratory, under contract No. F61775-01-WE004 to C. Haldoupis, and by the National Science and Engineering Research Council (NSERC) of Canada through an operating grant to G. C. Hussey. We wish to thank both reviewers for their constructive comments.

[44] Arthur Richmond thanks Don Moorcroft and John D. Sahr for their assistance in evaluating this paper.

References

Balsley, B. B., and D. T. Farley, Radar studies of the equatorial electrojet in three frequencies, *J. Geophys. Res.*, *76*, 8341, 1971.

Buneman, O., Excitation of field aligned sound waves by electron streams, *Phys. Rev. Lett.*, *10*, 285, 1963.

Cosgrove, R. B., and R. T. Tsunoda, Polarization electric fields sustained by closed-current dynamo structures in midlatitude sporadic *E*, *Geophys. Res. Lett.*, *28*, 1455, 2001.

Ecklund, W. L., D. A. Carter, and B. B. Balsley, Gradient drift irregularities in mid-latitude sporadic *E*, *J. Geophys. Res.*, *86*, 858, 1981.

Farley, D. T., A plasma instability resulting in field-aligned irregularities in the ionosphere, *J. Geophys. Res.*, *68*, 6083, 1963.

Farley, D. T., Theory of equatorial electrojet waves: New developments and current status, *J. Atmos. Terr. Phys.*, *47*, 729, 1985.

Farley, D. T., and B. G. Fejer, The effect of the gradient drift term on Type 1 electrojet irregularities, *J. Geophys. Res.*, *80*, 3087, 1975.

Farley, D. T., and J. Providakes, The variation with T_e and T_i of the velocity of unstable ionospheric two-stream waves, *J. Geophys. Res.*, *94*, 15,415, 1989.

Fejer, B. G., and M. C. Kelley, Ionospheric irregularities, *Rev. Geophys*, *18*, 401, 1980.

Fejer, B. G., J. Providakes, and D. T. Farley, Theory of plasma waves in the auroral *E* region, *J. Geophys. Res.*, *89*, 7487, 1984.

Haldoupis, C., A review of radio studies of auroral *E* region ionospheric irregularities, *Ann. Geophys.*, *7*, 239, 1989.

Haldoupis, C., and K. Schlegel, Direct comparison of 1-m irregularity phase velocities and ion acoustic speeds in the auroral *E* region ionosphere, *J. Geophys. Res.*, *95*, 18,989, 1990.

Haldoupis, C., and K. Schlegel, A 50-MHz radio Doppler experiment for midlatitude *E* region coherent backscatter studies: System description and first results, *Radio Sci.*, *28*, 959, 1993.

Haldoupis, C., K. Schlegel, and D. T. Farley, An explanation for type 1 echoes from the midlatitude *E*-region ionosphere, *Geophys. Res. Lett.*, *23*, 97, 1996.

Haldoupis, C., D. T. Farley, and K. Schlegel, Type 1 echoes in the midlatitude *E* region, *Ann. Geophys.*, *15*, 908, 1997.

Huang, C.-M., Midlatitude type 1 echoes observed with the Chung-Li 52 MHz radar, *J. Atmos. Sol. Terr. Phys.*, *62*, 751, 2000.

Hussey, G. C., K. Schlegel, and C. Haldoupis, Simultaneous 50-MHz coherent backscatter and digital ionosonde observations in the midlatitude *E* region, *J. Geophys. Res.*, *103*, 6991, 1998.

Hysell, D. L., and J. D. Burcham, The 30-MHz radar interferometer studies of midlatitude *E* region irregularities, *J. Geophys. Res.*, *105*, 12,797, 2000.

Kelley, M. C., *The Earth's Ionosphere: Plasma Physics and Electrodynamics*, Academic, San Diego, Calif., 1989.

Kissack, R. S., J.-P. St.-Maurice, and D. R. Moorcroft, Electron thermal effects on the Farley-Buneman fluid dispersion relation, *Phys. Plasmas*, *2*, 1032, 1995.

Kissack, R. S., J.-P. St.-Maurice, and D. R. Moorcroft, The effect of electron-neutral energy exchange on the fluid Farley-Buneman instability threshold, *J. Geophys. Res.*, *102*, 24,091, 1997.

Koehler, J. A., C. Haldoupis, K. Schlegel, and V. Virvilis, Simultaneous observations of *E* region coherent radar echoes at 2-m and 6-m radio wavelengths at midlatitude, *J. Geophys. Res.*, *102*, 17,255, 1997.

Koehler, J. A., C. Haldoupis, and K. Schlegel, Coherent backscatter cross-section ratio measurements in the midlatitude *E* region ionosphere, *J. Geophys. Res.*, *104*, 4351, 1999.

Lacroix, P. J., and D. R. Moorcroft, Ion acoustic HF radar echoes at high latitudes and far ranges, *J. Geophys. Res.*, *106*, 29,091, 2001.

Leadabrand, R. L., J. C. Schlobohm, and M. J. Baron, Simultaneous very high frequency and ultra high frequency observations of the aurora at Fraserburgh, Scotland, *J. Geophys. Res.*, *70*, 4235, 1965.

Lee, K., C. F. Kennel, and J. M. Kindel, High frequency Hall current instability, *Radio Sci.*, *6*, 209, 1971.

Milan, S. E., and M. Lester, A classification of spectral populations observed in HF radar backscatter from the *E* region auroral electrojets, *Ann. Geophys.*, *19*, 189, 2001.

Moorcroft, D. R., Wavelength dependence of electrostatic plasma wave propagation in the auroral *E* region, *J. Geophys. Res.*, *92*, 3423, 1987.

Moorcroft, D. R., and J. M. Ruohoniemi, Nearly simultaneous measurements of radar auroral heights and Doppler velocities at 398 MHz, *J. Geophys. Res.*, *92*, 3333, 1987.

Nielsen, E., and K. Schlegel, Coherent radar Doppler measurements and their relationship to the ionospheric electron drift velocity, *J. Geophys. Res.*, *90*, 3498, 1985.

Ossakow, S. L., K. Papadopoulos, J. Orens, and T. Coffey, Parallel propagation effects on the type 1 electrojet instability, *J. Geophys. Res.*, *80*, 141, 1975.

Pfaff, R. F., M. Yamamoto, P. Marionni, H. Mori, and S. Fukao, Electric field measurements above and within a sporadic-*E* layer, *Geophys. Res. Lett.*, *25*, 1769, 1998.

Riggin, D., W. E. Swartz, J. F. Providakes, and D. T. Farley, Radar studies of long-wavelength waves associated with midlatitude sporadic *E* layers, *J. Geophys. Res.*, *91*, 8011, 1986.

Sahr, J. D., and B. G. Fejer, Auroral electrojet plasma irregularity theory and experiment: A critical review of present understanding and future directions, *J. Geophys. Res.*, *101*, 26,893, 1996.

Schlegel, K., Interpretation of auroral radar experiments using a kinetic theory of the two stream instability theory, *Radio Sci.*, *18*, 108, 1983.

Schlegel, K., The influence of metallic ions on the plasma instabilities in the high latitude *E* region, *Radio Sci.*, *20*, 740, 1985.

Schlegel, K., and C. Haldoupis, Observation of the modified two-stream plasma instability in the midlatitude *E*-region ionosphere, *J. Geophys. Res.*, *99*, 6219, 1994.

Schlegel, K., and J.-P. St.-Maurice, Short wavelength gradient-drift waves at high latitudes, *Ann. Geophys.*, *1*, 259, 1983.

Schlegel, K., T. Turunen, and D. R. Moorcroft, Auroral radar measurements at 16-cm wavelength with high range and time resolution, *J. Geophys. Res.*, *95*, 19,001, 1990.

Schmidt, M. J., and S. P. Gary, Density gradients and the Farley-Buneman instability, *J. Geophys. Res.*, *78*, 8261, 1973.

Shalimov, S., C. Haldoupis, and K. Schlegel, Large polarization electric fields associated with midlatitude sporadic *E*, *J. Geophys. Res.*, *103*, 11,617, 1998.

St.-Maurice, J.-P., and A. M. Hamza, A new nonlinear approach to the theory of *E* region irregularities, *J. Geophys. Res.*, *106*, 1751, 2001.

Stubbe, P., Theory of electrostatic waves in an *E* region plasma, *J. Geophys. Res.*, *94*, 5303, 1989.

Tsunoda, R. T., On polarized frontal structures, type 1 and quasi-periodic echoes in midlatitude sporadic *E*, *Geophys. Res. Lett.*, *25*, 2641, 1998.

C. Haldoupis, Physics Department, University of Crete, Iraklion, Crete, 71003 Greece. (chald@physics.uoc.gr)

G. C. Hussey and J. A. Koehler, Institute of Space and Atmospheric Studies, Department of Physics and Engineering Physics, University of Saskatchewan, 116 Science Place, Saskatoon, SK, Saskatoon S7N-5E2, Canada. (hussey@usask.ca; koehler@dansas.usask.ca)

K. Schlegel, Max-Planck Institut für Aeronomie, Katlenburg-Lindau, D-37191 Germany. (schlegel@linmpi.mpg.de)

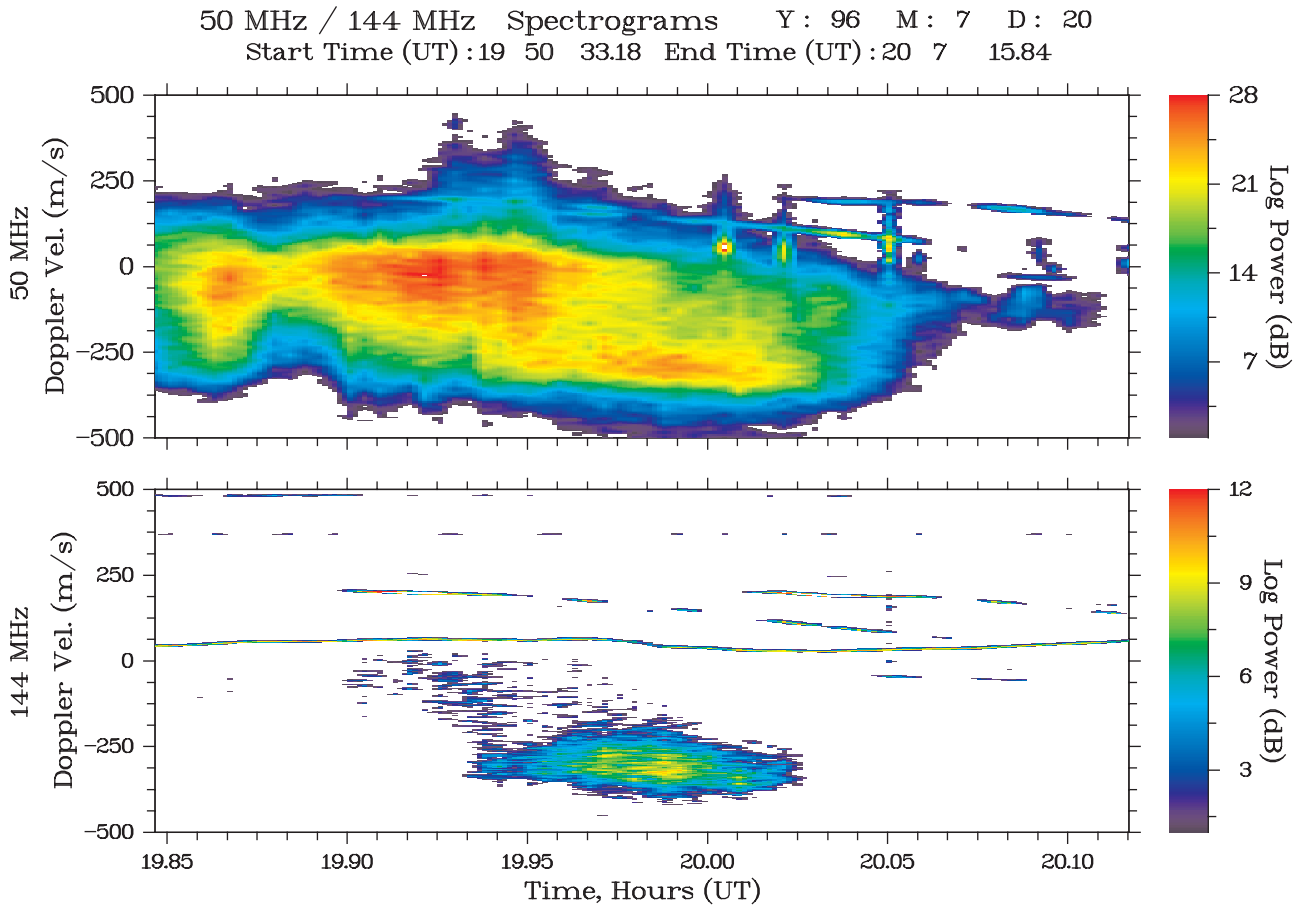

Figure 2. Simultaneous Doppler spectrograms of coherent backscatter at 50 MHz (top) and 144 MHz (bottom). Seen here is a typical event of type 1 echoes, characterized by large negative Doppler velocities and narrow spectra, seen concurrently in both radar frequencies. The time axis is in decimal hours UT (local time LT = UT + 1.6 hours). The long narrow lines are either due to antenna sidelobe airplane reflections or interference. Note also that type 2 echoes (broad spectra centered at lower Doppler shifts) dominate the spectrogram at 50 MHz but they are nearly absent at 144 MHz.